Sensitivity Analysis of Strong Cyclone Track Deflection over Isolated Topography: Exploring the Impact of Vortex Impinging Direction and Strength

Hung-Cheng Chen [1,*]

[1] School of Education, Huanggang Normal University, Hubei, China;

* Correspondence: hungcheng@hgnu.edu.cn

† Presented at the 6th International Electronic Conference on Atmospheric Sciences, 15-30 October 2023 Available online: https://ecas2023.sciforum.net

Abstract: This study performs a sensitivity analysis of strong cyclone track deflection over isolated topography, exploring the impacts of vortex impinging direction and strength. A dynamic model investigates track adjustments of cyclonic vortices on a β-plane. The study derives a meridional adjustment velocity (MAV) for vortex motion and examines variations in track patterns under different flow conditions. Results reveal an S-shaped pattern in most tracks and significant deflections when the vortex passes over high-rise terrain. Larger direction angles of the vortex result in more pronounced deflections attributed to the terrain loop effect induced by the strong topographic β effect. Adjacent vortex paths impinging from the south converge on the leeward side, improving prediction accuracy, while vortices crossing from the north diverge, reducing prediction accuracy. This study offers valuable insights into uncertainties associated with path prediction.

Keywords: tropical cyclone; path prediction; track deflection; dynamic model; sensitivity analysis; cyclone-terrain interaction

1. Introduction

The interaction between strong geophysical vortices and topography has been extensively studied, with a particular focus on tropical cyclones encountering terrain. Shieh et al. [1] and Wang [2] studied over 200 tropical cyclones threatening Taiwan and classified them into different categories based on their movement patterns. These studies revealed the presence of local northwest rule, where cyclones tend to deflect southward as they approach the mountains due to the combined effect of blocking and channeling [3]. The local northwest rule governing vortex propagation over topography was demonstrated in rotating tank experiments by Carnevale et al. [4]. They showed that barotropic vortices follow the local topographic slope, reflecting a balance between planetary and topographic β effects. Zavala Sansón and van Heijst [5] extended this concept, identifying combinations of vortex and topographic parameters dictating scattering or trapping.

According to Lin [6], terrain-induced wind asymmetries near vortex cores cause downstream track deflections. Idealized simulations by Lin and Savage [7] quantified the dependence on landfall location, elucidating the dynamics of track discontinuities when Taiwan's CMR is encountered. Recent modeling by Huang and Wu [8] isolated the impact of elliptical idealized islands on upstream cyclone steering, showing terrain geometry strongly influences steering direction. Rotating tank experiments from Chen et al. [9-10] examined vortex structure changes over topography, providing physical insights complementing numerical simulations.

The above reviews highlight the complexity of vortex interactions with topography and their impact on the track deflection of tropical cyclones. The local northwest rule, characterized by the southward deflection of cyclones as they approach mountains, plays a crucial role in this phenomenon. Studies have identified various factors, such as basic flow Froude number, blocking, channeling, and asymmetric flow, contributing to the track deflection. Further research using laboratory experiments and numerical simulations has provided valuable insights into the essential dynamics of vortex-terrain interactions.

This study presents a comprehensive sensitivity analysis of cyclone track deflection over isolated topography, focusing on the impact of vortex impinging direction and strength. A dynamic model is used to investigate the track adjustment of strong cyclonic vortices on a β-plane in an isolated topographic feature. The analysis reveals an S-shaped pattern in most tracks, characterized by a southward deflection on the windward side and a northward recovery on the lee side of the vortex motion. The study highlights the challenges in accurately predicting the path of tropical cyclones when they encounter high-rise features in the terrain.

2. Dynamic Model of Strong Cyclones over Topography

The present study employs the dynamical model proposed by Chen et al. [11] to analyze the trajectories of strong cyclonic vortices passing through terrain. This model, based on the conservation principle of potential vorticity under the shallow water framework, predicts the dimensionless drift velocity of the vortices as $\vec{V}^* \approx \vec{V_i}^* + \vec{V_y}^*$, where $\vec{V_i}^*$ represents the initial drift velocity of the vortices unaffected by terrain effects, and $\vec{V_y}^*$ denotes the meridional adjusted velocity (MAV), defined as follow:

$$\vec{V_y}^* = -\alpha \frac{\mathrm{d}h_B^*}{\mathrm{d}t^*} \vec{e_y} \tag{1}$$

where the topographic modification factor α is defined as

$$\alpha = \left(1 + Ro_v \zeta_c^*\right) \beta_B^* \big/ \beta_0^*. \tag{2}$$

Equation (2) includes four dimensionless parameters: the vortex Rossby number Ro_v, relative vorticity at vortex center ζ_c^*, planetary Beta number β_0^*, and topographic Beta number β_B^*. The definitions of these parameters can be found in Chen et al. [11].

3. Results and Discussion

In this study, a dynamic model was employed to predict the path of a typhoon-like vortex impinging a three-dimensional idealized bell-shaped mountain, with reference to the geometric conditions of Taiwan's terrain. The position and topographic features of the mountain were determined as

$$h_B = h_M \left(1 + \left(\frac{x-x_a}{a_h}\right)^2 + \left(\frac{y-y_a}{b_h}\right)^2\right)^{-3/2}. \tag{3}$$

where x_a and y_a represent the center coordinates of the mountain, and a_h and b_h denote the half-widths of the mountain in the x and y directions, respectively. Referring to Lin's research [3], values consistent with the characteristics of Taiwan's Central Mountain Range (CMR) were adopted: $h_M = 3\ km$, x_a approximately 121°E longitude, y_a approximately 23.5°N latitude, $a_h = 40\ km$, and $b_h = 120\ km$.

Additionally, an idealized moderate-strength typhoon-like vortex (denotes as Vortex M) is initialized with the following conditions: maximum wind radius $R_m = 150\ km$, maximum wind speed $V_m = 40\ m/s$, mean relative vorticity at the center $\zeta_c = 4 \times 10^{-4}\ s^{-1}$, and undisturbed water depth $D = 10\ km$. The dynamic model employs an integration time step of 150 seconds. It's noteworthy to mention that the impinging angle, γ, of the vortex is defined as the angle between the initial drift direction of the vortex and

the normal direction of the terrain's central axis. The track deflection of the vortex δ depicts the latitudinal path difference influenced by the terrain.

3.1. Vortex Trajectories, Drifting Speed and Track Deflection of Vortex M

Figure 1 displays the spatiotemporal evolution of trajectories, drifting speeds, and track deflections for Vortex M making landfall over terrain from various approach angles. Figures 1(a) to 1(d) correspond to vortex impinging angles of 195°, 170°, 150°, and 130°, respectively. For each impinging angle, we compute three paths traversing the terrain through the northern, central, and southern regions with a latitude spacing of 1.375 degrees. In this study, the reference lines were set at 24.5°N and 22.5°N, categorizing paths above 24.5°N as the northern landfall path, between 22.5°N and 24.5°N as the central landfall path, and below 22.5°N as the southern landfall path.

The paths of the vortex exhibit varying degrees of S-shaped curves due to the influence of MAV. Specifically, on the windward side, the MAV points southward, resulting in a southward deflection of the path. Conversely, on the leeward side, the MAV points northward, leading to a northward deflection. The red hollow circles and blue crosses in Figure 1 represent the locations of the minimum MAV (pointing southward) and maximum MAV (pointing northward) along each vortex path, respectively.

When the vortex impinging angle is held constant, the results show that the degree of path deflection is correlated with variations in terrain topography. In regions with steep terrain in the central area, the vortex exhibits a larger deflection. Conversely, in relatively flat terrains in the northern and southern regions, the vortex displays smaller deflections. Additionally, as the vortex impinging angle decreases, the deflection through the central terrain increases, reaching a maximum deflection of approximately 238 km southward (refer to the deflection plots in Figure 1(d)). Considering the variations in vortex propagation speed, the landfall path through the central terrain demonstrates significant acceleration, particularly when passing over mountains, where the vortex near the mountaintop reaches a speed of 8.84 m/s (Figure 1(a)). As the vortex impact angle decreases, the velocity near the mountaintop decreases to 6.04 m/s (Figure 1(d)).
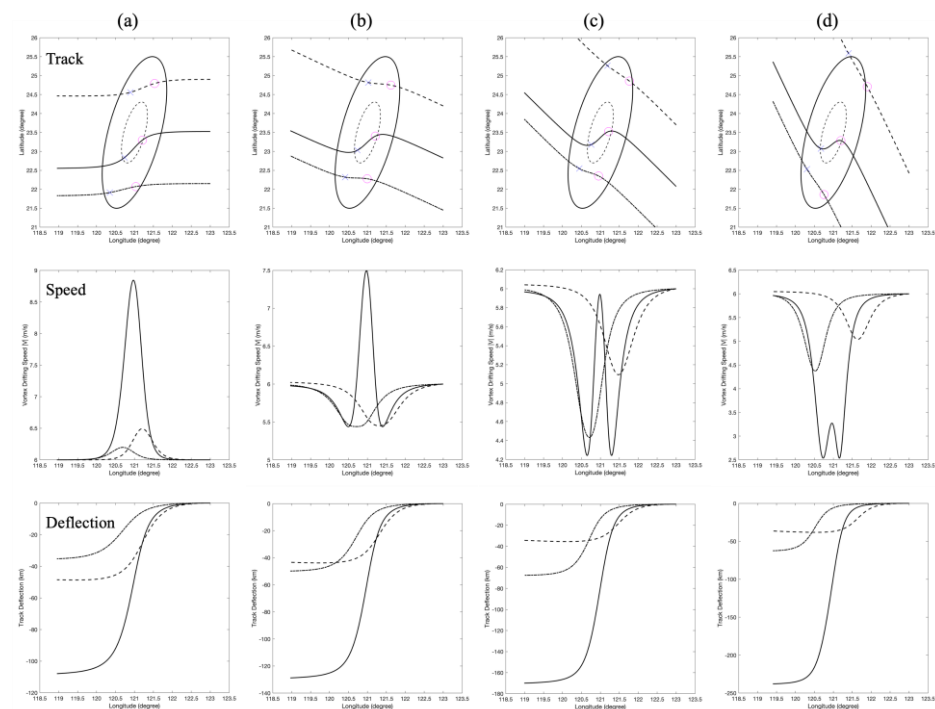

Figure 1. Vortex trajectories, drifting speed, and track deflection of Vortex M making landfall over terrain.

3.2. Effect of Vortex Impinging Direction

Figure 2 displays the multiple trajectory paths for a Vortex M making landfall over terrain from varying approach directions. Figures 2(a) to 2(d) correspond to vortex impinging angles of 195°, 170°, 150°, and 130°, respectively. For each impinging angle, 31, 31, 31, and 46 vortex trajectories are computed, respectively, with initial path spacing of approximately 13.88 km.

Examining the variations in the distances between neighboring vortex paths, it is found that the paths north of the boundary track (BT), defined as the path passing through the mountain summit, exhibit a diverging phenomenon after traversing the mountain crest. Conversely, paths south of BT demonstrate converging behavior, with stronger convergence for tracks closer to BT. As the impinging angle decreases, the divergence and convergence of adjacent paths becomes increasingly pronounced. For the 130° multi-track case (Figure 2d), the maximum separation reaches 58.11 km, 4.19 times the initial 13.88 km spacing. Meanwhile, the minimum converges to 2.68 km, 20% of the initial path interval.

The significance of the above pre- and post-mountain variations in adjacent pathways can be summarized regarding path predictability and sensitivity. The divergence north of BT signifies increasing forecast uncertainty after crossing the mountain crest. From another perspective, initial pre-mountain path prediction errors (as represented by the interval of adjacent paths) amplify downstream. The uncertainty is higher for paths closer to the boundary track. In contrast, the convergence south of BT denotes decreasing path forecast uncertainty across the mountain. Initial path prediction errors shrink downstream, with higher prediction accuracy for tracks approaching BT.
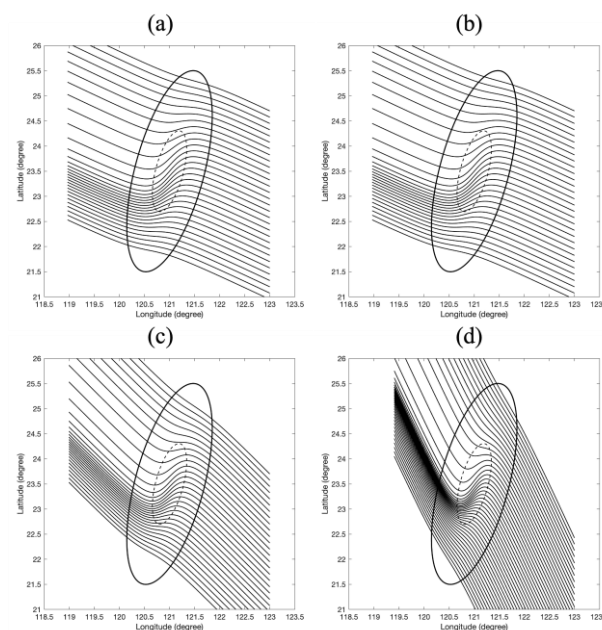

Figure 2. Multiple trajectory paths of Vortex M making landfall over terrain from varying impinging angles of (a) 195°, (b) 170°, (c) 150°, and (d) 130°, respectively.

3.3. Effect of Vortex Strength

Figure 3 illustrates the multiple trajectory paths depicting the landfall of four vortices with varying intensities and structures, generated under a fixed vortex propagation direction (vortex impinging angle of 170 degrees). These vortices are initiated with an approximate initial path spacing of 13.88 km. Table 1 provides a detailed listing of these four vortices, denoted as Vortex A through Vortex D, along with their structural parameters.

Observing the variations in the distances between adjacent vortex paths, we note that with the increase in the average relative vorticity of the vortices, the divergence and convergence phenomena mentioned in the previous section become more pronounced. It is worth noting that in the multiple trajectory paths of Vortex D (see Figure 3d), the calculated 31 vortex paths did not proceed over the terrain obstacle on the windward side but instead deflected southward, ultimately converging within a very narrow region in the southwest area of the terrain. This resulted in a reduction of the minimum path spacing to 0.35 km, which corresponds to 2.5% of the initial path spacing.

Table 1. Strength and structure of four vortices.

Vortex	R_m (km)	V_m (m/s)	ζ_c (1/s)
A	150	30	4×10^{-4}
B	100	30	6×10^{-4}
C	150	60	8×10^{-4}
D	100	60	1.2×10^{-3}

The phenomenon of the vortex deflecting southward around the terrain can be regarded as a manifestation of the local northwest rule. However, strong vortex-terrain interactions often induce secondary vortices which can alter the primary vortex track. Further validation against complete flow field calculations (e.g., shallow water models) is therefore needed to verify the applicability of the dynamic model in such cases [11]. The emergence of secondary vortices and their potential impacts on the pathways merit dedicated investigation in future studies.
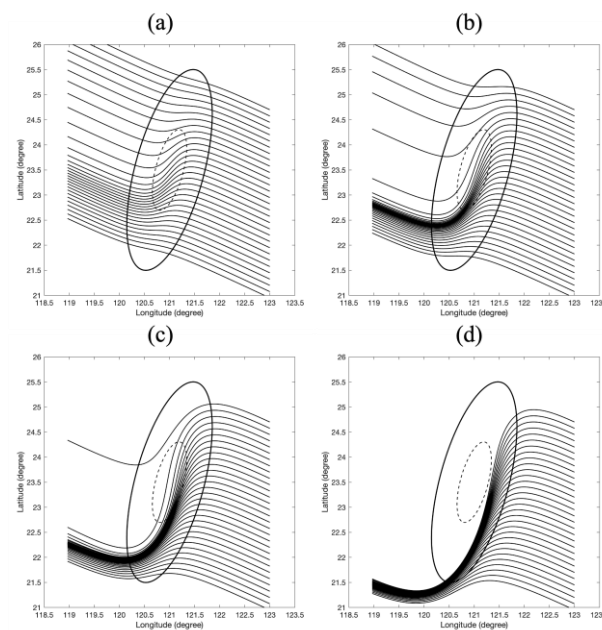

Figure 3. Multiple trajectory paths of four vortices with varying strength making landfall over terrain from vortex impinging angle of 170°. (a) Vortex A, (b) Vortex B, (c) Vortex C, and (d) Vortex D.

4. Conclusions

This study utilized a dynamic model to perform a sensitivity analysis of strong cyclone track deflections over isolated topography. By systematically varying the vortex impinging direction and strength, the model results revealed complex nonlinear relationships governing the trajectory adjustments and identified key factors influencing path predictability. Firstly, the study reveals that cyclonic vortices experience significant deflection when encountering high-rise terrain, with larger impinging angles leading to

more pronounced deflections. This is attributed to the terrain loop effect induced by the strong topographic β effect. Secondly, the spatiotemporal evolution of vortex trajectories demonstrates an S-shaped pattern, with the meridional adjustment velocity (MAV) influencing the southward deflection on the windward side and northward deflection on the leeward side.

Thirdly, the study highlights the importance of vortex impinging direction in predicting cyclone paths. The paths north of the boundary track (BT) exhibit divergence after crossing the mountain crest, indicating increasing forecast uncertainty. Conversely, paths south of BT demonstrate convergence, enhancing prediction accuracy. Analysis of adjacent tracks in the results further elucidated predictability sensitivities, with divergence amplifying downstream errors on the windward side while convergence improved accuracy on the leeward side. Lastly, the impact of vortex strength is explored, showing that vortices with higher average relative vorticity exhibit more pronounced divergence and convergence phenomena. Notably, Vortex D deflects southward around the terrain, converging in a narrow region, which can be attributed to the local northwest rule.

Overall, this study provides valuable insights into the sensitivity of cyclone track deflection over isolated topography, contributing to a better understanding of path prediction uncertainty and the need for further investigations into vortex-terrain interactions. While requiring further validation, this initial sensitivity analysis highlighted the model's capabilities in assessing terrain-adjusted cyclone steering and associated forecast uncertainties under varied scenarios. Future refinement of model physics and expanded analyses can provide valuable insights into cyclone-terrain interactions and prediction challenges relevant to real-world tropical systems.

Institutional Review Board Statement: Not applicable.

Informed Consent Statement: Not applicable.

Data Availability Statement: Data is unavailable due to privacy or ethical restrictions.

Conflicts of Interest: The authors declare no conflict of interest.

References

1. Shieh, S.L.; Wang, S.T.; Cheng, M.D.; Yeh, T.C. Tropical cyclone tracks over Taiwan and its vicinity for the one hundred years 1897 to 1996 (in Chinese). Research Rep. CWB86-1M-01, Central Weather Bureau, Taipei, Taiwan, 1997; pp. 497.
2. Wang, S.T. An integrated study of the impact of the orography in Taiwan on the movement, intensity, structure, wind and rainfall distribution of invading typhoons (in Chinese). Technical Rep. 80-73, Chinese National Science Council, Taipei, Taiwan, 1992; pp. 285.
3. Lin, Y.L.; Han, J.; Hamilton, D.W.; Huang, C.Y. Orographic influence on a drifting cyclone. *J. Atmos. Sci.* **1999**, *56*, 534–562.
4. Carnevale, G.; Kloosterziel, R.; Van Heijst, G. Propagation of barotropic vortices over topography in a rotating tank. *J. Fluid Mech.* **1991**, *233*, 119–139.
5. Zavala Sansón, L.; Heijst, G.J.F.V. Interaction of barotropic vortices with coastal topography: Laboratory experiments and numerical simulations. *J. Phys. Oceanogr.* **2000**, *30*, 2141–2162.
6. Lin, Y.L. *Mesoscale Dynamics*; Cambridge University Press: Cambridge, UK, 2007; pp. 630.
7. Lin, Y.L.; Savage, L.C., III. Effects of landfall location and the approach angle of a cyclone vortex encountering a mesoscale mountain range. *J. Atmos. Sci.* **2011**, *68*, 2095–2106.
8. Huang, K.C.; Wu, C.C. The impact of idealized terrain on upstream tropical cyclone track. *J. Atmos. Sci.* **2018**, *75*, 3887–3910.
9. Chen, H.C.; Leu, J.H.; Liu, Y.; Xie, H.S.; Chen, Q. A Validated Study of a Modified Shallow Water Model for Strong Cyclonic Motions and Their Structures in a Rotating Tank. *Math. Probl. Eng.* **2021**, *2021*, 5529601.
10. Chen, H.C.; Leu, J.H.; Lin, Y.L.; Liu, H.P.; Huang, C.L.; Chen, H.S.; Lan, T.S. Cyclonic motion and structure in rotating tank: Experiment and theoretical analysis. *Sens. Mater.* **2021**, *3*, 2385–2395.
11. Chen, H. C., Chu, C. C., & Chang, C. C. A dynamic model for strong vortices over topography on a β plane. *Advances in Engineering Mechanics-Reflections and Outlooks-In Honor of Theodore Y. T. Wu.*; World Scientific Publishing Company: Singapore, 2005; pp. 669-680.